May, 1986] *Bull. Chem. Soc. Jpn.*, *59*, *1443—1448 (1986)* 1443

Phase Transition of Quaternary Alkyl Halide Salts of 1,4-Diazabicyclo[2.2.2]octane

Jun Shimizu, Kengo Imamura, Takashi Nogami,* and Hiroshi Mikawa†
Department of Applied Chemistry, Faculty of Engineering, Osaka University,
Yamada-oka, Suita, Osaka 565
(Received November 12, 1985)

A series of quaternary alkyl halide salts of 1,4-diazabicyclo[2.2.2]octane (DABCO) exhibited first-order phase transitions in the temperature range of 62—100 °C. Abrupt changes of halide anion conductivities were observed by two to three orders of magnitude at the transition temperatures. The transition temperature and the heat of transition tend to increase with the increase of the alkyl chain length. The temperature dependence of an IR spectrum showed that the band progressions due to long alkyl chain disappeared above the phase transition. This fact suggests that the *trans*-zigzag conformation of alkyl chains in the low temperature phase is destroyed by the internal rotation of the alkyl chain above the transition temperature.

Long-chain alkanes and their derivatives have attracted much attention for more than 50 years since the work by Müller.¹⁾ He discovered a solid-state phase transition at a few degrees below the melting point. It has now been established that the phase transition is to be attributed to the hindered rotation of the alkyl chains.²⁾ The solid-state phase transition between an ordered phase (low temperature phase) and a rotator phase (high temperature phase) is interesting in relation to the melting process of polymer crystals as well as to the similar phase transition of some membranes (phospholipids).³⁾ The theoretical work on this problem before 1965 was surveyed by McClure.⁴⁾ Phase transitions involving conformational change were also observed for some *n*-alkanes.⁵⁾ Knowledge of the various types of polymethylene motions has accumulated substantially in the past few years, since the problems have been tackled both theoretically⁶⁾ and experimentally⁷⁾ with various independent techniques.

Independent of the above subjects, we have been studying halide anion conductivities by using several organic materials such as crown ether complexes,⁸⁾ cryptand complexes,⁹⁾ quaternary alkylammonium halides,¹⁰⁾ and quaternary alkylphosphonium halides.¹¹⁾ As an extention of these studies, we have investigated the halide anion conductivities of a series of quaternary alkyl halide salts of 1,4-diazabicyclo[2.2.2]octane (DABCO), and found a first-order phase transition with concomitant and abrupt changes of the halide anion conductivities and crystal structures.¹²⁾ It has now been clarified that the phase transition in the present systems is to be attributed to the internal rotation of the C–C bonds of the alkyl chains in the solid state. Unlike alkanes and their derivatives, the phase transition temperature of the DABCO salts are more than one hundred degrees below their melting points (or decomposition points). This paper describes more details of the phase transition of the DABCO salts from the viewpoints of halide anion conductivities, thermal analyses, infrared absorption spectroscopy, and observations with a polarization microscope. The names of the quaternary alkyl halide salts of DABCO in the present study are abbreviated by the numbers of carbons of alkyl chains and the kinds of anions. For example, *N*,*N*′-didodecyl-1,4-diazoniabicyclo[2.2.2]octane dibromide is abbreviated as C_{12}–DABCO–Br. The materials studied are shown in Fig. 1.

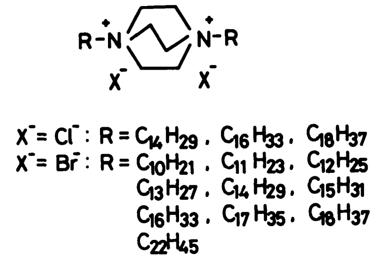

Fig. 1. Quaternary alkyl halide salts of DABCO.

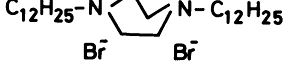

C_{12}-DABCO-Br

Experimental

Materials. Methyl alcohol was distilled without any drying procedures. Acetonitrile was passed through a column composed of several layers of basic, neutral, and acidic aluminas, refluxed over calcium hydride overnight, and then distilled. DABCO and all of alkyl halides were used without purifications.

Syntheses of Quaternary Alkyl Halide Salts of DABCO.

---

† Present address: Department of Environment and Safety Engineering, Faculty of Engineering, Fukui Institute of Technology, Gakuen-cho, Fukui 910.

Synthesis of quaternary alkyl halide salt of DABCO is described for C_{12}–DABCO–Br as a typical example. A methanol solution (30 ml) of DABCO (1.68 g, 15 mmol) and dodecyl bromide (7.48 g, 30 mmol) was refluxed for 36 h, and then allowed to cool to room temperature. It was then poured into benzene (500 ml) to obtain a white precipitate. It was filtered, dried, and then recrystallized three times from acetonitrile to obtain crystals of thin rectangular plates. For the chloride salts, acetonitrile was used as a reaction medium, and the reaction was conducted for 96 h. For the iodide salts, the same reaction conditions as described in the above example were adopted. In some cases, powders precipitate when the solution was cooled to room temperature after the reaction. In this case, a hot homogeneous solution was poured into benzene to obtain a precipitate. The solvents of recrystallization are as follows: acetonitrile for bromide salts possessing alkyl chains of C_{10}–C_{14}, and all of the chloride salts; ethyl alcohol for C_{14}–DABCO–I, C_{16}–DABCO–I, and bromide salts possessing longer alkyl chains than C_{14}

Measurements. Ionic conductivities were measured by a vector impedance meter 4800A (Hewlett Packard) in the frequency range of 25 Hz—500 kHz. Since all of the samples were hygroscopic, they were handled in a glove box until they were transferred to a glass vessel. The sample was compressed to a pellet (13 mm of diameter and ca. 0.5 mm of thickness) by applying a pressure of 300 kg cm^{-2} and sandwiched between platinum plates. After setting it was transferred to a sample holder made of Teflon, it was mounted in a glass vessel, dried under dynamic vacuum at 80 °C overnight, cooled to room temperature, and then subjected to measurement. After the drying procedure, the contribution of the proton conduction due to moisture seems to be negligible. Differential scanning calorimetry measurements of the samples were made on a SSC-560S (Daini Seikousha Co. Ltd) calorimeter with a scanning speed of 5 °C min^{-1}. The temperature dependence of the infrared spectra was measured by an A-102 (Japan Spectroscopic Co. Ltd.) for a KBr disk sample. The sample holder was surrounded by a ribbon heater.

Results and Discussion

Halide Anion Conductivities. All of the samples have already been confirmed as halide anion conductors.[12,13] Ionic conductivities were measured by an AC method. The impedance and a phase shift were measured, and the real and imaginary parts of the impedance were plotted for various frequencies (25 Hz—500 kHz). The impedance plot for C_{12}–DABCO–Br thus obtained at 78 °C is shown in Fig. 2 as a typical example. A semicircular arc was obtained in the high frequency range, which indicates that the equivalent circuit of the impedance is approximated by a parallel connection of a resistance and a capacitance. The linear relation with a 45° slope in the low frequency range might be due to a Warburg impedance. The resistance of the sample was estimated from the extrapolation of the semicircular arc to an abscissa. Temperature dependences of halide anion conductivities were measured with raising the temperature of the sample slowly from a room temperature; they are shown in Fig. 3 ((a) for chlorides, (b) for bromides, and (c) for iodides). Conductivities less than 10^{-9} S cm^{-1} are below the limit of our measurements. The following facts are noteworthy from this figure. (1) All of the samples show abrupt increases of the ionic conductivities by two to three orders of magnitude within narrow temperature ranges; this is attributed to a first-order phase transition as described later. (2) The order of the transition temperatures (T_c) of chlorides, bromides, and iodides is $Cl^- < Br^- < I^-$, when the carbon numbers of alkyl groups are fixed. (3) The longer the alkyl chains, the higher are the T_c, although a few exceptions are found.[14] (4) The order of the ionic conductivities of chlorides, bromides, and iodides is $Cl^- > Br^- > I^-$. (5) The longer the alkyl chain, the lower is the halide anion conductivity below T_c. However, the halide anion conductivities are close to each other above T_c; these points will be discussed later.

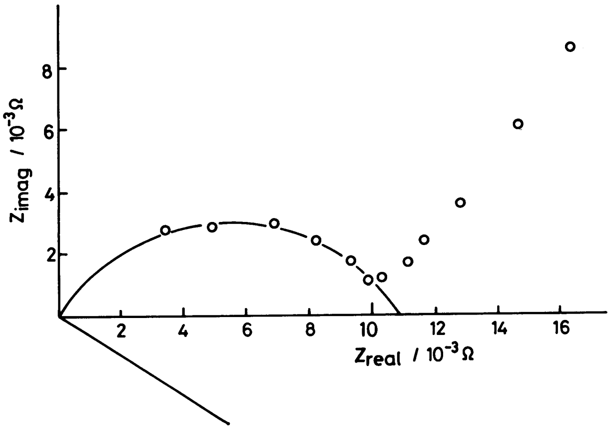

Fig. 2. The plots of the real and imaginary parts of impedance of C_{12}–DABCO–Br (a compressed pellet sample with an electrode area of 1.33 cm^2 and a thickness of 0.346 mm) at 78 °C in the frequency range of 25 Hz—500 kHz.

The close correspondence between T_c's and the lengths of the alkyl chains suggests that the phase transition is closely related to the structure of the alkyl group. The order of the ionic conductivities among three halides are due to the anionic size; the bigger the anionic size, the lower is its conductivity. Part of Table 1 shows materials, and the ratios of halide anion conductivities before (σ_l) and after (σ_h) the phase transition, i.e., σ_h/σ_l. The changes of the conductivities at T_c were found to be in the range of 150—180 for chloride salts, 630—3600 for bromide salts, and 140—350 for iodide salts. The abrupt change of the ionic conductivity showed hysteresis phenomena. Figure 4 shows the experimental results

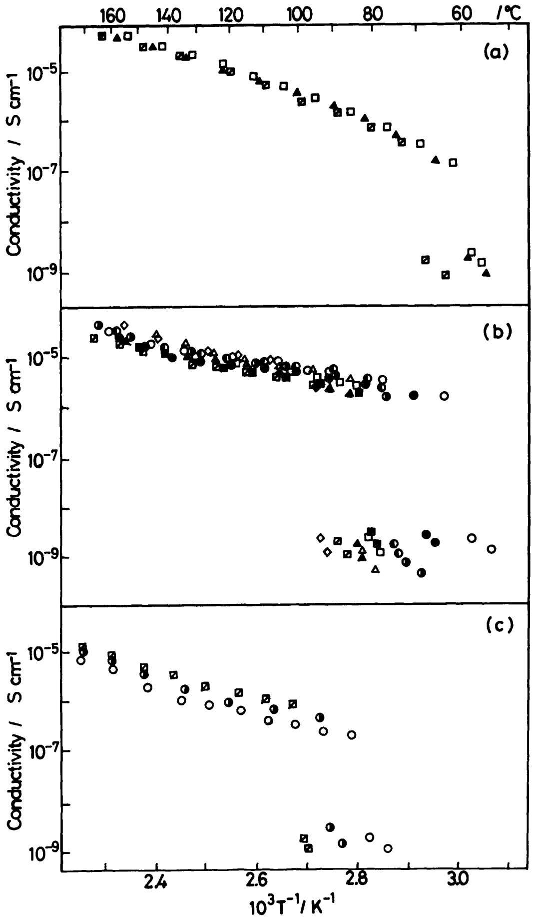

Fig. 3. Temperature dependences of halide anion conductivities.
(a) Chloride salts:
□: C_{14}–DABCO–Cl, ▨: C_{16}–DABCO–Cl, ▲: C_{18}–DABCO–Cl.
(b) Bromide Salts:
○: C_{10}–DABCO–Br, ●: C_{11}–DABCO–Br, ◑: C_{12}–DABCO–Br, ◐: C_{13}–DABCO–Br, □: C_{14}–DABCO–Br, ■: C_{15}–DABCO–Br, ▨: C_{16}–DABCO–Br, △: C_{17}–DABCO–Br, ▲: C_{18}–DABCO–Br, ◇: C_{22}–DABCO–Br.
(c) Iodide salts:
○: C_{10}–DABCO–I, ◑: C_{12}–DABCO–I, ▨: C_{16}–DABCO–I.

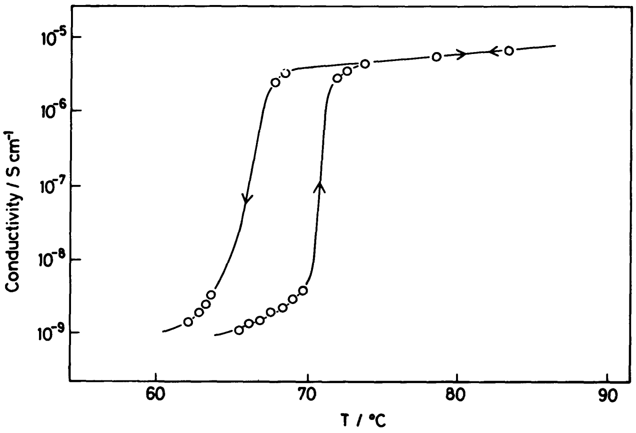

Fig. 4. Hysteresis of bromide anion conductivities of C_{12}–DABCO–Br.

Table 1. Quaternary Alkyl Halide Salts of DABCO, Phase-Transition Temperatures (T_c), Ratios of Halide Anion Conductivities Before (σ_l) and After (σ_h) Transition, and Endothermic (Q_{en}) and Exothermic (Q_{ex}) Heats of Transition

Materials	T_c[a]		σ_h/σ_l	Q_{en}	Q_{ex}
	°C			kJmol^{-1}	kJ mol^{-1}
(a) Chloride salts					
C_{14}–DABCO–Cl	61	51	150	41.4	38.5
C_{16}–DABCO–Cl	73	62	190	65.3	67.4
C_{18}–DABCO–Cl	61	53	180	68.7	71.2
(b) Bromide salts					
C_{10}–DABCO–Br	64	57	850	45.2	41.4
C_{11}–DABCO–Br	72	69	630	48.1	45.6
C_{12}–DABCO–Br	76	69	920	71.2	68.2
C_{13}–DABCO–Br	83	76	1500	67.4	62.8
C_{14}–DABCO–Br	88	78	1400	85.8	83.7
C_{15}–DABCO–Br	92	83	980	80.4	75.8
C_{16}–DABCO–Br	92	88	1200	96.3	101.7
C_{17}–DABCO–Br	96	86	3600	93.8	85.6
C_{18}–DABCO–Br	93	91	1400	105.5	105.9
C_{22}–DABCO–Br	99	96	2200	116.0	117.2
(c) Iodide salts					
C_{10}–DABCO–I	87	85	140	40.2	41.0
C_{12}–DABCO–I	93	91	190	54.8	53.2
C_{16}–DABCO–I	103	101	350	91.3	86.7

[a] The temperatures in the left and right columns indicate the T_c's observed by heating and cooling the samples, respectively.

of C_{12}–DABCO–Br as an example, when the temperature was elevated above T_c and then cooled down again.

Differential Scanning Calorimetries. DSC measurements of the salts showed an endothermic transition at T_c when the temperature was elevated from room temperature across the T_c. An exothermic transition was observed at T_c when the temperature was lowered after it had been raised above T_c. Table 1 also shows T_c's and the endothermic (Q_{en}) and the exothermic (Q_{ex}) heats of transition. Owing to the hysteresis phenomenon, two T_c's are shown for each material. They were obtained by the onset of DSC peaks. The transition temperatures observed by heating the sample were, in general, higher than those observed by cooling the sample. The differences of the two T_c's were found to be in the range of 8—11 °C for chloride salts, 2—10 °C for bromide salts, and 2 °C for iodide salts. Figure 5 shows plots of the transition temperatures against the

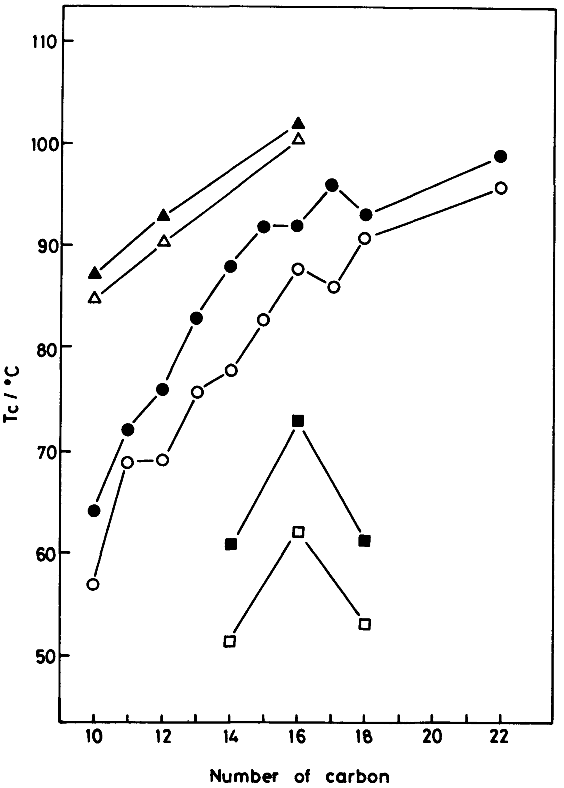

Fig. 5. Plots of phase transition temperatures against the number of carbons of alkyl group. The two transition temperatures of each material were obtained by the onset of the DSC peaks when the temperature was elevated or lowered across T_c's. The T_c's observed by heating the samples are higher than those observed by cooling the sample, and they are plotted independently. □, ■: chloride, ○, ●: bromide, △, ▲: iodide.

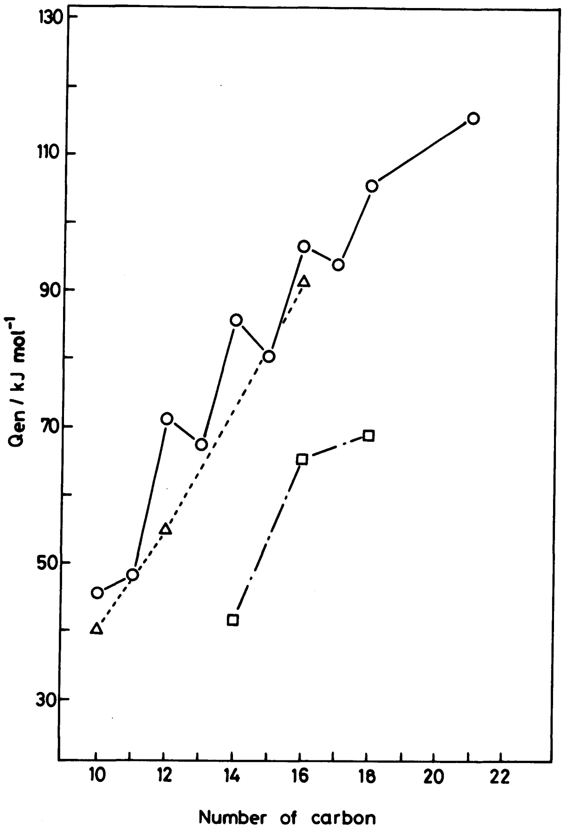

Fig. 6. Plots of endothermic heats of transition against the number of carbons of alkyl group. □: chloride, ○: bromide, △: iodide.

number of carbon atoms of the alkyl group attached to the DABCO nitrogen. This figure shows two T_c's for each material, corresponding to that observed by heating the sample and that observed by cooling. It is noteworthy that an even-odd number effect of carbons on the transition temperature was found for bromide salts in Fig. 5. The same type of effect on the phase transition temperature was also observed for a series of long chain alkanes and alcohols.15) In most materials, the endothermic heats of transition were slightly larger than the exothermic heats of transition; this point will be discussed later. Figure 6 shows the plots of the endothermic heats of transition against the carbon numbers of the alkyl groups. This figure shows only the endothermic heats of transition, because they seem to represent the latent heats between the two phases more correctly than the exothermic heats of transition as described later. The heats of transition tend to increase as the alkyl group chains become longer. This suggests that the main factor controlling the transition is the change of the conformation of the alkyl chain. The order of the heats of transition of chlorides, bromides, and iodides is $\mathrm{Br^- > I^- > Cl^-}$, if the number of carbon atoms in the alkyl group is fixed. It is noteworthy that an excellent even-odd number effect is observed for bromide salts as shown in Fig. 6.15)

Infrared Absorption Spectroscopy. The temperature dependence of the infrared absorption spectra was measured to obtain more information on the phase transition. Figure 7 shows the temperature dependence of the IR spectra of C_{14}-DABCO-Br measured for a KBr disk sample at 30 and 100 °C as an example. The absorptions shown by the solid and dotted arrows at 30 °C are assumed to be due to band progressions,16) which are well-known for long alkanes.18) Many band progressions were smeared out at 100 °C. Detailed measurements revealed that this change of the absorption occurred exactly at the transition temperature. The disappearance of several band progressions in the high temperature range indicates that the *trans*-zigzag conformation of the alkyl chain in the low temperature phase is destroyed by the internal rotation of the C–C bonds of alkyl chain above the transition temperature.19) Thus, the phase transition observed for DABCO salts is an order-disorder type.

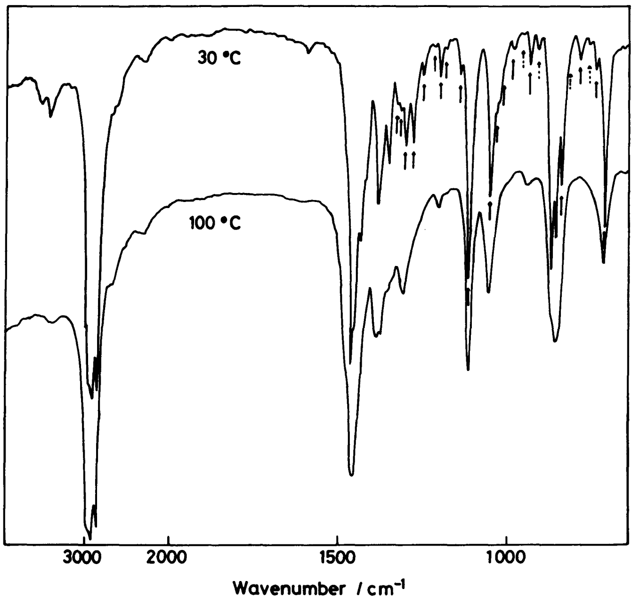

Fig. 7. Infrared absorption spectra of C_{14}–DABCO–Br for the KBr disk sample at 30 °C and 100 °C. The absorptions shown by the solid and dotted arrows at 30 °C are assigned to band progressions of the CH_2 vibrational mode.

Observation by Polarization Microscope. The above conclusion was also supported by observing the sample crystal in a polarization microscope under crossed Nicols condition. The bright transmitted light in the low temperature phase disappeared almost completely at the transition temperature, and the situation was unchanged even if the crystal were rotated above T_c. The abrupt decrease of the transmitted light above T_c reflects the lack of anisotropy of the crystal[20] due to the internal rotation of the C–C bonds of the alkyl chain.

Miscellaneous Discussions. The fact that the ionic conductivities become lower with the increase of the alkyl chain length below T_c is explained as follows. Judging from the crystal shapes of DABCO salts (very thin and rectangular) and from the crystal structures of related compounds,[21] the DABCO salts seem to possess layered structures, in which the long axes of the molecules are parallel with each other. The ion transport perpendicular to the long axis of a molecule seems not to be influenced so much by the length of the alkyl chain. On the other hand, the ion transport parallel to the long axis of the molecule will be retarded by the increase of the alkyl chain length, because the ion hopping length between anionic sites becomes longer. Thus, the latter effect accounts for the experimental observations. The reason why the ionic conductivities above T_c were similar to each other is as yet not clear. However, the following factors may be operative. The channel of the halide anion transport is greatly influenced by the packing of the individual molecule in the crystal. Since the material converts to the disordered phase above T_c, the peculiar pathway in the low temperature phase, which is closely related to the length of the molecule, and/or to the packing of molecules in the solid, would be destroyed or averaged by the movement of the alkyl group to give a structure-insensitive situation for anion transport.

The facts that the endothermic heats of transition are slightly larger than the exothermic heats of transition in most materials would be explained as follows. The former is caused by the transition from the ordered phase to the disordered phase. On the other hand, the latter is caused by the reverse transition. However, the disorder of the alkyl chain remains to some extent in the latter case, which gives rise to smaller exothermic heats of transition. This is consistent with the microscope observation that the surface of the crystal was wrinkled when the temperature was raised and lowered several times across T_c. Thus, the endothermic heat of transition seems to correspond to the latent heat between the ordered phase and the disordered phase more correctly than the exothermic heat of transition.

Summary. In conclusion, we have found that a series of quaternary alkyl halide salts of DABCO show first-order phase transitions, with concomitant and abrupt changes of halide anion conductivities, and infrared absorption spectra. The transition is caused by the change of the conformation of the alkyl group, possibly by the internal rotation of the C–C bonds of the alkyl chains. Therefore, the phase transition in the present study is closely related to the phase transitions of alkanes and their derivatives. The most distinct difference of the DABCO salts from others is that the transition temperatures are more than 100 degrees lower than the melting points (or decomposition points), because the latter are usually above 200 °C. The reason is that the present DABCO salts are ionic materials, and the lattice is more rigid than that of long alkanes and their derivatives which are covalent materials. The abrupt changes of the halide anion conductivities and the absence of birefringence above the transition temperature may be applicable to thermal switching devices. In this case, an output signal can be obtained both by electrical and optical techniques. The large differences between the transition temperatures and the melting points (or decomposition points) are favorable for such a device, because it ensures stability.

The authors are grateful to Professor Masamichi Kobayashi, Department of Macromolecular Science, Faculty of Science, Osaka University, for his discussions on the phase transitions of alkanes and on the assignment of the infrared absorption spectra of the present study. We are also grateful to Professor

Shigekazu Kusabayashi and Dr. Shunsuke Takenaka for the use of the DSC and the polarization microscope.

References

1) A. Müller, *Proc. Roy. Soc. (London),* **A138**, 514 (1932).

2) J. D. Hoffmann, *J. Chem. Phys.,* **20**, 541 (1952).

3) D. A. Pink, T. J. Green, and D. Chapman, *Biochemistry,* **19**, 349 (1980).

4) D. W. McClure, *J. Chem. Phys.,* **49**, 1830 (1968).

5) R. G. Snyder, M. Maroncelli, H. L. Strauss, C. A. Ellinger, D. G. Cameron, H. L. Casal, and H. H. Mantsch, *J. Am. Chem. Soc.,* **105**, 133 (1983).

6) M. Kobayashi, *J. Chem. Phys.,* **68**, 145 (1978).

7) G. Zerbi, R. Magni, M. Gussoni, K. H. Horitz, A. Bigotto, and S. Dirlinkov, *J. Chem. Phys.,* **75**, 3175 (1981).

8) M. Fujimoto, T. Nogami, and H. Mikawa, *Chem. Lett.,* **1982**, 547.

9) M. Fujimoto, T. Nogami, and H. Mikawa, *Solid State Ionics,* **11**, 313 (1984).

10) J .Shimizu, T. Nogami, and H. Mikawa, *Solid State Ionics,* **14** 153 (1984).

11) K. Imamura, T. Nogami, and H. Mikawa, *Solid State Ionics,* **17**, 77 (1985).

12) J. Shimizu, T. Nogami, and H. Mikawa, *Solid State Commun.,* **54**, 1009 (1985).

13) A charge carrier was determined as a bromide or an iodide anion by a DC technique, using a graphite pellet electrode containing tetrabutylammonium tribromide or tetrabutylammonium triiodide (see Ref 12). In the case of the quaternary alkyl chloride salts of DABCO, we could not use the same technique, because of the instability of tetrabutylammonium trichloride. Judging from the similarity of the materials, however, the charge carrier of the chloride salts would be a chloride anion.

14) The exceptions were found for chloride salts and C_{17}–DABCO–Br.

15) A. A. Schaerer, C. J. Busso, A. E. Smith, and L. B. Skinner, *J. Am. Chem. Soc.,* **77**, 2017 (1955); A. Watanabe, *Bull. Chem. Soc. Jpn.,* **36**, 336 (1963).

16) The peak positions of the solid arrows are in fairly good accordance with the band progressions of n-$C_{15}H_{32}$, which have the same numbers of CH_2 units as the alkyl group of C_{14}–DABCO–Br. For the detailed assignments of the band progressions, see Ref. 17. The absorptions shown by the dotted arrows are due to the band progressions possessing the phase difference (ϕ_k) between adjacent CH_2 units given by $\phi_k = k\pi/14$, where k is an even number. These bands become IR-active because of the lower symmetry of the alkyl group of C_{14}–DABCO–Br than n-$C_{15}H_{32}$. The assignments of the band progressions in Fig. 7 have some ambiguities in the range of 1170—1310 cm^{-1}, because both the CH_2 wagging and CH_2 twisting-rocking modes have absorptions in this range. Since single absorption was observed at 720 cm^{-1} (CH_2-rocking mode) in Fig. 7, C_{14}–DABCO–Br seems to possess a parallel-packed molecular structure in the crystal. In this case, crystal field splitting does not appear. The separations of the absorptions shown by the arrows are too large to be the crystal field splittings, because these are usually less than 10 cm^{-1}.

17) R. G. Snyder and J. H. Schachtschneider, *Spectrochim. Acta,* **19**, 85 (1963).

18) H. Tadokoro, "Structure of Crystalline Polymers," Wiley Interscience, New York (1979), pp. 304—311.

19) J. R. Nielsen and C. E. Hathaway, *J. Mol. Spectroscopy,* **10**, 366 (1963). M. R. Barr, B. A. Dunell, and R. F. Grant, *Can. J. Chem.,* **41**, 1188 (1963).

20) Since the sample shows some powdered X-ray diffraction patterns above the transition temperature (see Ref. 12), the high temperature phase is not completely amorphous.

21) M. Kobayashi, T. Kobayashi, Y. Itoh, and K. Sato, *J. Chem. Phys.,* **80**, 2897 (1984).